

LETTERS

A Remarkable Elevation of Freezing Temperature of CCl₄ in Graphitic Micropores

Katsumi Kaneko,* Ayumi Watanabe, Taku Iiyama, Ravi Radhakrishnan,† and Keith E. Gubbins†

Physical Chemistry, Material Science, Graduate School of Science and Technology, Chiba University, 1-33 Yayoi, Inage, Chiba 263-8522, Japan and Chemical Engineering, North Carolina State University, 113 Riddick Labs, Raleigh, North Carolina 27695-7905

Received: March 4, 1999; In Final Form: June 29, 1999

The freezing behavior of CCl₄ confined in graphitic micropores of activated carbon fibers (ACFs) was examined by use of differential scanning calorimetry over the temperature range of 180 to 320 K. For ACF of average pore width, $w = 1.1$ nm, we observed a clear peak showing that the freezing temperature is 299 K. The freezing temperature was elevated by 57 K. However, the enthalpy of freezing was only 1.0% of that of the bulk liquid CCl₄ to an fcc solid phase. CCl₄ confined in micropores of $w = 0.80$ nm had a more diffuse DSC peak, providing a similar elevation of the freezing temperature and an even smaller freezing enthalpy of 0.5% of the bulk value.

Introduction

The structure and phase behavior of molecular assemblies confined in small pores have attracted much attention. Freezing and melting of condensates in mesopores have been studied for a long time.¹ Recently, well-defined porous materials have led to an active study on the phase behavior of confined fluids.^{2–5} In almost all cases a clear depression of the freezing temperature was observed, and the depression has been basically explained by the capillary effect in surface chemistry. Recent experimental and molecular simulation studies have shown that the classical capillary theory is not enough.^{6–8} Miyahara and Gubbins⁸ simulated freezing and melting phenomena for a Lennard–Jones model of CH₄ in graphitic slit pores. They showed that the freezing temperature is elevated relative to that of the bulk liquid; the increase is greater for smaller pores, but the freezing disappears in small micropores.^{7,8} This predicted elevation of freezing in porous carbons has recently been reconfirmed by

careful free energy calculations by Radhakrishnan and Gubbins.⁹ However, we do not have sufficient experimental data on the phase behavior of fluids confined in micropores for understanding this phenomenon. Organized structures have been reported for CCl₄,^{10,11} H₂O,¹² SO₂,¹³ and O₂¹⁴ in micrographitic slit micropores of activated carbon fiber (ACF), which change with the slit width. Hence, the micropores of ACFs can offer a good system for studying the freezing effect in confined structures. The structures of CCl₄ in ACF micropores at 303 K were examined by in situ X-ray diffraction and GCMC simulation, showing that the CCl₄ molecular assembly structure depends on the pore width.^{10,11} Also, the freezing of bulk CCl₄ had been studied using a calorimetric method and X-ray diffraction.^{15–18} Information on bulk CCl₄ should be helpful for understanding CCl₄ in micropores.

This letter reports a marked elevation of the freezing temperature of CCl₄ in micrographitic micropores.

Experimental and Simulation Section

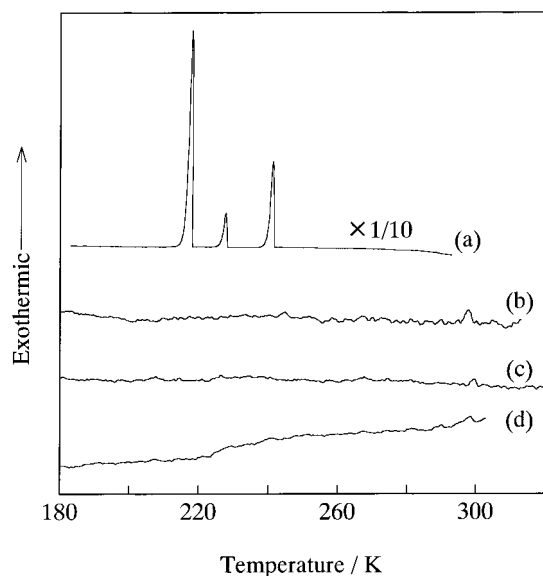
Pitch-based ACFs of different pore widths (P5, P10, and P20) were used as the micrographitic micropore system. The mi-

* Corresponding author: Department of Chemistry, Faculty of Science, Chiba University, 1-33 Yayoi, Inage, Chiba 263-8522, Japan. Fax +81-43-290-2779; tel +81-43-290-2788; e-mail kaneko@pchem2.s.chiba-u.ac.jp.

† North Carolina State University.

TABLE 1: Micropore Structure of ACF Samples by N₂ Adsorption

	micropore vol (mL g ⁻¹)	surface area (m ² g ⁻¹)	pore width (nm)
P5	0.336	900	0.75
P10	0.622	1510	0.82
P20	0.970	1770	1.13

**Figure 1.** DSC cooling curves of CCl₄ confined in micropores of various ACFs and of bulk CCl₄ liquid: (a) bulk liquid, (b) P20, (c) P10, and (d) P5. Here the ordinate scale of bulk liquid is reduced by 1/10.

cropore volume, the specific surface area, and the slit pore width were determined by the high-resolution N₂ adsorption isotherm at 77 K using a subtracting pore effect method.^{19,20} Table 1 lists the micropore structural parameters. The pore widths were in the range of 0.75 to 1.1 nm. CCl₄ was adsorbed at 303 K under a saturated vapor pressure after drying ACF samples by evacuation at 373 K for 2 h. The ACF samples with adsorbed CCl₄ were sealed in an aluminum pan. The DSC chart was recorded at the temperature scanning rate of 5 K min⁻¹ or 1 K min⁻¹ using a DSC system (MAC Science, DSC3100). We repeated measurements of the DSC cooling or heating charts three times and summed them to obtain the average DSC curve. The freezing temperature was determined by the crossing point of the linear rising part of the peak and the average background. The enthalpy of freezing was obtained from the peak area. The melting temperature was determined using the dropping linear part of the peak.

The interaction between the adsorbed fluid molecules is modeled using the Lennard–Jones potential with the one-center parameters $\sigma_{ff} = 0.514$ nm and $\epsilon_{ff}/k_B = 366$ K. This potential reproduced the correct melting temperature for bulk CCl₄. We used regular slit graphite pores to describe the micropores of ACF. The adsorption of CCl₄ in the graphite slit pore was calculated using GCMC simulation at different temperatures for different pore widths. The Landau free energy was calculated for the GCMC simulated adsorption isotherm, and this was used to determine the phase transition temperature.²¹ The detailed simulation method will be published elsewhere.²²

Results and Discussion

Figure 1 shows the DSC cooling charts for CCl₄ confined in micropores of ACFs at 303 K. The DSC chart for the bulk CCl₄

TABLE 2: Amounts of CCl₄ Adsorbed in Micropores of ACF and DSC Data

	adsorbed CCl ₄ (mg g ⁻¹)	freezing temp (K)	ΔH_s^a (J mol ⁻¹)	melting temp (K)	ΔH_m^a (J mol ⁻¹)
P5	330	300	5	299	3
P10	555	301	8	300	14
P20	1470	299	17	298	20
bulk liquid		242	1570		
bulk solid				248	2190

^a Here, ΔH_s and ΔH_m denote the enthalpies of freezing and melting, respectively. The enthalpy of melting of bulk CCl₄ in the literature is 2.56 kJ mol⁻¹.

liquid is also shown in Figure 1 for comparison. The DSC chart of the bulk liquid has three sharp peaks. The heat evolution peaks which are ascribed to the liquid to fcc solid phase (I_a) transition, the I_a to rhombohedral phase (I_b) transition, and the I_b to monoclinic phase (solid_m) transition begin at 241.8 K, 228.4 K, and 218.3 K, respectively. These transition temperatures in the literature are 242–250 K, 231–242 K, and 225 K for the liquid–I_a, I_a–I_b, and I_b–solid_m transitions, respectively.^{16–18} The observed transition temperatures are close to the literature values, although the correct determination of the phase transition temperature is difficult from the cooling curve because of supercooling. The peak of the I_b–solid_m transition is the most intense. On the other hand, only one diffuse peak of the heat evolution for CCl₄ confined in micropores of ACF is observed around 300 K, which is much higher than that of the bulk liquid. This peak should come from the freezing of CCl₄ confined in micropores, although three peaks are not observed, as in the bulk CCl₄. The strong confinement of CCl₄ molecules in the micropores should prohibit ordinary solid-phase transitions. The DSC peak for the P20 micropore material is more evident than those for the P10 and P5 materials. The freezing temperature of CCl₄ for P20 is 299 K, being higher than that of bulk CCl₄ by 57 K. Also, the freezing temperatures for P10 and P5 are estimated to be 301 and 300 K, respectively, from the quite diffuse noisy peak; in particular, the determination of the freezing temperature of P5 is quite difficult owing to strong diffuseness. The enthalpy of freezing, ΔH_s , for the confined CCl₄ is much smaller than that of the bulk liquid, and the ΔH_s values are listed in Table 2. The ΔH_s of the confined CCl₄ becomes smaller with decreasing pore width, while the freezing temperature does not vary significantly with the pore width.

Figure 2 shows the DSC curves of CCl₄ confined in micropores of P20 upon cooling (a) and heating (b). The heating curve of bulk solid CCl₄ is shown for comparison, which has two peaks at 223 and 248 K originating from the solid_m–I_b and I_b–liquid transitions.¹⁸ Figure 2 shows both the remarkable elevation of the melting temperature of confined CCl₄ by 50 K and the markedly small enthalpy of melting. There is no meaningful difference between the freezing and melting temperatures of confined CCl₄. The enthalpy of melting of confined CCl₄ is quite small compared with the bulk value, as is the enthalpy of freezing. Thus, the melting temperature of confined CCl₄ is much higher than that of bulk CCl₄ liquid. DSC measurements upon heating were carried out on other ACF samples; similar tendencies were observed, as shown in Table 2. The melting temperature of confined CCl₄ does not depend on the pore width, but the enthalpy of melting becomes smaller with decreasing the pore width in a similar way to the freezing behavior.

The features of the observed DSC results on CCl₄ confined in graphitic micropores of which micropore width is less than 1.2 nm are as follows. The elevation of the freezing temperature

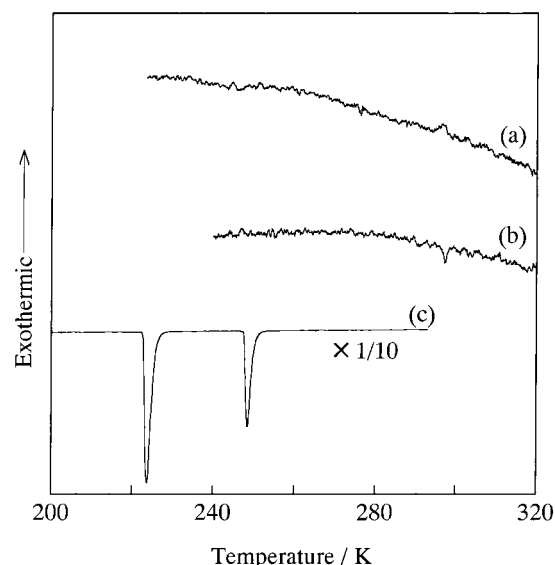


Figure 2. Averaged DSC curves of CCl_4 confined in micropores of P20 on cooling and heating. The heating curve of bulk CCl_4 solid, whose ordinate is reduced to 1/10, is shown: (a) cooling and (b) heating curves of confined CCl_4 , (c) heating curve of bulk CCl_4 .

is about $58 (\pm 1)$ K, which does not sensitively depend on the pore width for this range of pore widths. The enthalpy of freezing is less than 1% of the bulk value. The melting of confined CCl_4 has a similar tendency to the freezing behavior. A confined liquid in mesopores should exhibit a depression of the freezing and melting temperatures according to classical surface chemistry.¹ The phase behavior of confined CCl_4 in carbon is quite unique, being different from those of liquid confined in most other materials. Miyahara and Gubbins⁸ proposed that if the interaction of a molecule with the sample pore surface is greater than that with the pore wall consisting of adsorbate molecules, the freezing temperature should be elevated with decreasing pore width and the freezing disappears in narrow micropores. The Lennard–Jones size parameter of CCl_4 is 0.5881 nm, and the intermolecular interaction is limited to the nearest neighbors. Hence, the interaction of a CCl_4 molecule with the wall made of CCl_4 molecules should be weaker than the interaction of a CCl_4 molecule with the graphitic pore wall. Therefore, the observed elevation of the freezing and melting temperatures for confined CCl_4 can be explained basically by the Miyahara and Gubbins theory. Iiyama et al. determined the electron radial distribution function of CCl_4 confined in micropores of ACFs at 303 K from the X-ray diffraction patterns, showing that the second-nearest neighbor peak of CCl_4 molecules shifts to a smaller side because of the more dense structure of confined CCl_4 and that the plastic crystalline structure, which is found at 253 K in the bulk phase,²² is formed in case of the pores of $w = 0.75$ nm.^{11,12} Thus, CCl_4 in micropores has an ordered structure similar to that of the solid even at 303 K on the basis of X-ray diffraction data,

coinciding with the observed DSC behavior. Hence, the freezing or melting temperature should be higher than the bulk value, as shown in this work. However, CCl_4 molecules in micropores cannot form a highly crystalline structure because of spatial restrictions. Also, even the liquid structure of confined CCl_4 should be more ordered than that of the bulk liquid. Thus the freezing of confined CCl_4 must be the transition of a partially ordered liquid to a highly defective solid; the enthalpy of freezing or melting in such a case is much smaller than the bulk value, as observed.

The simulation of the freezing of CCl_4 in a graphite slit showed that the freezing temperature is elevated by 90 K for pores of $w = 1.1$ nm (corresponding to P20). The upward shift obtained by the simulation is greater than the observed value. However, the agreement is reasonable regardless of the simple model. The simulation suggested the phase transition of the crystal phase to the orientationally ordered fluid upon freezing for confined CCl_4 in micropores of ACF, being consistent with the observed small enthalpy.

So far we have no direct structural information on the phase transition across the observed transition temperature using X-ray diffraction measurements. We hope to provide such data in the future after improvement of our X-ray diffraction system.

Acknowledgment. This work was supported by a grant-in-aid for Scientific Research on Priority Areas No. 288 (09243102) Carbon Alloys, Japanese Government and a grant from the National Science Foundation (Grant CTS-9896195), U.S.A. Government.

References and Notes

- (1) Defay, R.; Prigogine, I.; Bellemans, A.; Everett, D. H. *Surface Tension and Adsorption*; Longmans: London, 1966; Chapter 15.
- (2) Jackson, C. L.; McKenna, G. B. *J. Chem. Phys.* **1990**, *93*, 9002.
- (3) Mu, R.; Malhotra, V. M. *Phys. Rev.* **1991**, *44B*, 4296.
- (4) Unruh, K. M.; Huber, T. E.; Huber, C. A. *Phys. Rev.* **1993**, *48B*, 9021.
- (5) Sliwinski-Bartokowiak, M.; Gras, J.; Sikorski, R.; Radhakrishnan, R.; Gelb, L.; Gubbins, K. E. *Langmuir*, in press.
- (6) Ravikovitch, P. I.; Domhanail, S. C. O.; Neimark, A. V.; Schuth, F.; Unger, K. K. *Langmuir* **1995**, *3*, 443.
- (7) Inoue, S.; Hanzawa, Y.; Kaneko, K. *Langmuir* **1998**, *14*, 3079.
- (8) Miyahara, M.; Gubbins, K. E. *J. Chem. Phys.* **1997**, *106*, 1.
- (9) Radhakrishnan, R.; Gubbins, K. E. *Mol. Phys.* **1999**, *96*, 1249.
- (10) Iiyama, T.; Nishikawa, K.; Suzuki, T.; Otowa, T.; Hijiriyama, M.; Nojima, Y.; Kaneko, K. *J. Phys. Chem.* **1997**, *101*, 3037.
- (11) Suzuki, T.; Kaneko, K.; Gubbins, K. E. *Langmuir* **1998**, *13*, 2545.
- (12) Iiyama, T.; Nishikawa, K.; Otowa, T.; Kaneko, K. *J. Phys. Chem.* **1995**, *99*, 10075.
- (13) Wang, Z.; Kaneko, K. *J. Phys. Chem.* **1998**, *102*, 2863.
- (14) Kanoh, H.; Kaneko, K. *J. Phys. Chem.* **1996**, *100*, 755.
- (15) Hicks, J. F. G.; Hooley, J. G.; Stephenson, C. C. *J. Am. Chem. Soc.* **1944**, *66*, 1064.
- (16) Morrison, J. A.; Richards, E. L. *J. Chem. Thermodyn.* **1976**, *8*, 1033.
- (17) Koga, Y.; Morrison, J. A. *J. Chem. Phys.* **1975**, *62*, 3359.
- (18) Bean, V. E.; Wood, S. D. *J. Chem. Phys.* **1980**, *72*, 5838.
- (19) Kaneko, K.; Ishii, C.; Ruike, M.; Kuwabara, H. *Carbon* **1992**, *30*, 1075.
- (20) Setoyama, N.; Suzuki, T.; Kaneko, K. *Carbon* **1998**, *36*, 1459.
- (21) Radhakrishnan, R.; Gubbins, K. E.; Watanabe, A. R.; Kaneko, K. *J. Chem. Phys.*, to be submitted.
- (22) Nishikawa, K.; Murata, K. *Bull. Chem. Soc. Jpn.* **1979**, *52*, 293.